4-7-2015

Elastic and electronic properties of Ti2Al(CxN1−x) solid solutions

Sitaram Aryal
University of Missouri-Kansas City

Ridwan Sakidja
University of Missouri-Kansas City

Lizhi Ouyang
Tennessee State University

Wai-Yim Ching
University of Missouri-Kansas City

Recommended Citation

Sitaram Aryal, Ridwan Sakidja, Lizhi Ouyang, Wai-Yim Ching, "Elastic and electronic properties of Ti2Al(CxN1−x) solid solutions", Journal of the European Ceramic Society, Volume 35, Issue 12, 2015, Pages 3219-3227, ISSN 0955-2219, https://doi.org/10.1016/j.jeurceramsoc.2015.03.023.

Elastic and Electronic Properties of $Ti_2Al(C_xN_{1-x})$ Solid Solutions

Sitaram Aryal[1,2], Ridwan Sakidja[1,3], Lizhi Ouyang[2], and Wai-Yim Ching[1#]

1. Department of Physics and Astronomy, University of Missouri-Kansas City, Kansas City MO, 64110 USA
2. Department of Mathematics and Physics, Tennessee State University, Nashville TN 37209 USA.
3. Department of Physics, Astronomy and Materials Science, Missouri State University, Springfield, MO, 65897 USA.

Corresponding author: Chingw@umkc.edu, Tel: 816-235-2503, Fax: 816-235-5221

Abstract

The elastic coefficients and mechanical properties (bulk modulus, shear modulus, Young's modulus and Poisson's ratio) of $Ti_2Al(C_xN_{1-x})$ continuous solid solutions for x from 0 to 1 are calculated using *ab initio* DFT methods on 4x4x1 supercell models. It is shown that the properties of these solid solutions do not vary linearly with x. Although the lattice constant *c* is almost constant for $x \leq 0.5$, *a* increases linearly. For $x > 0.5$, *c* starts to increase with x while the rate of increase in *a* slows down. For x between 0.5 and 0.85, the elastic coefficients and the mechanical parameters show interesting dependence on x and crossovers, signifying the complex interplay in the structure and properties in $Ti_2Al(C_xN_{1-x})$ solid solutions. The nonlinear variations in mechanical properties are explained in terms of subtle difference in the electronic structure and bonding between nitrides and carbides in complex MAX phase compounds.

Key words: MAX phases, Solid Solutions,$Ti_2Al(C_{1-x}N_x)$, Mechanical properties, Electronic Structure.

1. Introduction

The transition metal ternary compounds $M_{n+1}AX_n$ or MAX phases with layered structures where X is either carbon or nitrogen has attracted great deal of attention in recent decades due to many of their fascinating properties and wide range of potential applications. Up to now, only about 70 of these phases are confirmed and synthesized [1]. Although the majority of these confirmed phases are 211 carbides with layer index n = 1, MAX phases with $n \geq 2$ also exist. Among the 211 phases, the most well-recognized phase is with M = Ti, A = Al and X = C, or Ti_2AlC. It has also been demonstrated that the formation of composite phases and solid solutions in MAX phases between different "M" elements, "A" elements and C and N are possible and well-documented. Such possibilities have greatly extended the range of compositions and in fine-turning the properties of MAX compounds. [1].

In spite of many papers published on the synthesis, properties and electronic structure calculations on MAX phases within last decades, one of the fundamental questions that still have eluded a clear answer is in what way the MAX carbides differ from nitrides, and why there has been far less nitrides synthesized in the laboratories than carbides?

Very recently, using a genomic approach, we presented a large data base on the elastic properties and electronic structure of 665 prescreened MAX phases [2]. Extensive trends, correlations in the mechanical and elastic properties, the electronic structure and bonding and trends in the progression of layered index *n* were explored and many noticeable differences between MAX carbides and nitrides were identified. We have also used this high quality data base to test and validate the data mining approach widely employed in materials informatics community [3]. However, no solid solution phases were included in our study which could significantly enlarge the data base for MAX phases. To our knowledge, there has been no accurate calculations on the MAX solid solutions mainly because such calculations will require large amount of computational resources. The only work that have been attempted appears to be a simplified calculation using quasi-harmonic Debye model for $Ti_2AlC_{0.5}N_{0.5}$ [4]. Solid solutions are no longer crystalline phases with well-defined long range order. They are essentially a class of disordered solids with random site substitutions. A sufficiently large number of supercells must be used to describe the structure and property variations with composition x.

Here, we report a detailed investigation on one of the most important MAX solid solution phases, $Ti_2Al(C_xN_{1-x})$. Ti_2AlC and Ti_2AlN are both well studied MAX phases and the transition from Ti_2AlC to Ti_2AlN or vice versa will be highly interesting because it may shed light on the source of the difference between MAX carbides and MAX nitrides. Their mechanical properties can be related to their parent mono-carbides and nitride TiC and TiN. There have also been speculation that solid solution phase can be a means to strengthen the MAX phases and alter its physical properties [1]. Finally, there are considerable amount of experimental studies on the $Ti_2Al(C_{-x}N_{1-x})$ solid solution albeit with limited x and relatively poor sample characterization [5-10]. Thus our *ab initio* calculations on the $Ti_2Al(C_xN_{1-x})$ solid solution is a timely effort to link computation to experimental efforts and in understanding some of the fundamental issues in MAX phases. More recently, MAX phase solid solutions of M site [11-15], A site [16, 17] and X site [18, 19] have been investigated by several research groups. Most of them focusing on the synthesis of the solid solution phases in the form of thin films, and few with large scale calculations. In particular, Yu and co-works [18] demonstrated that $Ti_2Al(C_xN_{1-x})$.solid solution can be synthesized in the entire composition range for x from 0 -1.0.

In this paper, we present the results of calculation on the elastic and mechanical properties of the $Ti_2Al(C_xN_{1-x})$ solid solutions using supercell models and detail their variation as a function of composition x in terms of the electronic structure and bonding as x changes. We briefly describe the supercell and computational methods employed in the next sections. The results for the solid solution are presented and discussed in Sections III. We end the paper with some conclusions.

2. Method and Model Construction

2.1 Supercell models

All calculations on the MAX $Ti_2Al(C_xN_{1-x})$ solid solutions were done a on 4 x 4 x 1 supercells each containing 128 atoms. Since MAX phases are elongated crystals with lattice parameter *c* much larger than *a*, the 4 x 4 x 1 supercell have lattice constant a = b close to c. (see **Fig. 1).** We constructed 17 models of different x including the end members Ti_2AlN (x = 0) and Ti_2AlC (x =

1) in the increment of Δx = 1/16. For each x (except the end members), 10 initial models with random distribution of C and N were constructed. These 10 models are then fully relaxed without constraints using the Vienna Ab initio Simulation Package (VASP) (see below). The model with the lowest total energy for each x is designated as the representative model structure for $Ti_2Al(C_xN_{1-x})$ solid solution at that x. The final representative models are further relaxed with higher precision as required for the elastic, mechanical and electronic structure calculations. To demonstrate that the sampling of 10 models for each x is more than adequate, we presented the mean energy, the lowest total energy, and standard deviation (σ) in Table 1. The standard deviation (σ) is also plotted against x and is shown in **Fig. 2.** As expected, σ is larger for x around 0.5 but is less than 0.20 eV which is extremely small (less than 0.02%), considering the mean values of the supercell total energy for x = 0.062, x = 0.50 and x = 0.938 are -1029.2296 eV, -1016.0403 eV and -1000.8834 eV respectively.

2.2 Methods used for relaxation and properties calculations

VASP[11] and OLCAO [12, 13] codes, both based density functional theory (DFT) based methods, are the primary tools used for the present calculations. VASP is used for relaxation of supercell models for each x and also for elastic properties calculations whereas OLCAO is exclusively used for electronic structure, bonding and optical conductivity calculations. In VASP, we used projector augmented wave (PAW)[14, 15] method and adopted the GGA PBE potential for exchange correlation functional as implemented in VASP[16, 17]. A high energy cutoff of 600 eV is used to ensure sufficient precision. We also used a rather stringent convergence criteria of 1.0 x 10^{-8} eV for electronic relaxation and 1.0 x 10^{-6} eV/Å for ionic force convergence. Since MAX phases are metals, a large Γ-centered, k-points mesh (3 × 3 × 3) for the supercell along with Methfessel-Paxton scheme for smearing are used to ensure high accuracy. Once the structures were fully relaxed with minimum internal stresses, we used the strain-stress analysis approach for elastic properties calculation[18, 19]. The stress tensor σ_{ij} under a set of applied strain ε_j are extracted and the elastic stiffness constants (C_{ij}) are obtained by solving tensorial equation $\sigma_{ij} = \sum_{ij} C_{ij}\varepsilon_j$. From the calculated C_{ij}, we obtain the bulk mechanical properties (bulk modulus K, shear modulus G, Young's modulus E and Poisson's ratio (η) using the well-tested Voight-Reuss-Hill (VRH) approximation for polycrystalline aggregates[20-22].

In OLCAO method [12, 13], we use atomic orbitals as the basis expansion and it is very efficient for large number of calculations with complex structures. Two most useful quantities in the OLCAO calculations are the effective charge Q* and bond order values between pairs of atoms using minimal basis given by the two equations below based on Mulliken scheme[23].

$$Q_\alpha^* = \sum_{i,\alpha}\sum_{n\ occ}\sum_{j,\beta} C_{i\alpha}^{*n} C_{j\beta}^{n} S_{i\alpha,j\beta} \quad (1)$$

$$\rho_{\alpha\beta} = \sum_{n,occ}\sum_{i,j} C_{i\alpha}^{*n} C_{j\beta}^{n} S_{i\alpha,j\beta} \quad (2)$$

where i, j label the orbital quantum number and n the band index, $C^{*}_{j\beta}$ are the eigenvector coefficients of the wave function and $S_{i\alpha,j\beta}$ is the overlap matrix between atoms α and β.
We have also calculated the optical conductivity $\sigma_1 = \varepsilon_{2(}\omega)\omega/4\pi$ for the $Ti_2Al(C_xN_{1-x})$ solid solution from the resulting wave functions according to [21]:

$$\varepsilon_2(\omega) = \left(\frac{e^2}{\pi m E \omega}\right) \times \int d\vec{k} \sum_{n,l} \left|\langle \psi_n(\vec{k},\vec{r}) \left|\vec{P}\right| \psi_n(\vec{k},\vec{r}) \rangle\right|^2 f_l(\vec{k}) \times \left[1 - f_n(\vec{k})\right] \delta\left[E_n(\vec{k}) - E_l(\vec{k}) - E\right] \quad (3)$$

The combination of VASP and OLCAO method in studying properties of different types of complex materials systems including metal[2, 24, 25], ceramics[26-29], and polymeric biomolecules[30, 31] and liquid and amorphous solids[32, 33] have been well demonstrated.

3. Results and Discussion

3.1 Elastic coefficient and mechanical parameters.

The calculated results for the elastic coefficients and mechanical parameters for $Ti_2Al(C_xN_{1-x})$ solid solution are listed in **Table 2**. Also included are the values of G/K ratio, aka Pugh moduli ratio. The results for the end members Ti_2AlN and Ti_2AlC agree with the experimental data and other calculations using unit cells. For example, the calculated bulk moduli of 160.67 GPa and 140.47 GPa for Ti_2AlN and Ti_2AlC are similar to our earlier calculations using unit cell and slightly lesser convergence criteria with values of 160.5 GPa and 139.7 GPa respectively[25]. The calculated elastic constants and other parameters agree quite well with other existing calculations[34, 35] and measured values [36, 37]. Before we discuss these results, we first present the variations in the supercell lattice constants and cell volume as a function of x which are shown in **Fig. 3** (a) and (b) respectively. At x = 0.5, our calculated lattice constants of *c* and *a* are 13.62 Å and 3.038 Å respectively which are in excellent agreement with the measured values of 13.610 Å and 3.023 Å respectively[7]. For $x \leq 0.5$, *a* increases linearly and *c* is almost constant. However, for $x > 0.5$, *c* starts to increase rather rapidly while the rate of increase in *a* shows marked slowing down. Obviously, there is a clear change in the lattice constants of the solid solution when the nitrogen content is below 50%. The supercell cell volume increases steadily as a function of x with its rate of increase slightly increased for x above 0.5.

Fig. 4 shows the variations of the elastic coefficients C_{ij} as a function of x. The C_{11} is always larger than C_{33} for all x showing the elastic anisotropy in the solid solution is maintained. However, it can be observed that C_{11} shows a shallow minimum at x = 0.56 and C33 flattens out after x = 0.60 and then decreases, a behavior closely related to the change in the variations of lattice constants *a* and *c* above x = 0.5.

The shear elastic constants (C_{44}, C_{66} and C_{12}, C_{13}) show more complex and interesting variations with x than the axial elastic coefficients C_{11} and C_{33}. The C_{44} and C_{66} are close to each other and much larger than the C_{13} and C_{12}. C_{44} is slightly larger than C_{66} on the lower side of x but they cross over at $x \sim 0.65$ after which C_{66} remains flat whereas C_{44} continue to decrease. C_{13} is considerably larger than C_{12} at low x but the crossover occurs at x = 0.815 above which they are very close to each other. The complex behavior of C_{ij} in $Ti_2Al(C_xN_{1-x})$ with respect to x is

astonishing without even considering other factors such as sub-stoichiometry, presence of vacancies and porosities which are common in MAX solid solutions samples.

In **Fig. 5(a),** we display the variations of bulk modulus K, Shear modulus G and Young's modulus E as a function of x in $Ti_2Al(C_xN_{1-x})$ solid solution. Since these moduli are derived from the C_{ij} values using VRH approximation, their variations with x will also be reflected in the plot but in a more averaged way. As expected, E is larger than K, and K is larger than G in that order. However, their variation patterns with x are not the same. They all show some marked transition region in the range roughly from x = 0.4 to x = 0.8. For example, the bulk modulus K shows it linearly decreases for x up to 0.5 whereas the shear modulus G appears to be constant for $x < 0.3$ and decreases from x between 0.3 and 0.6 and then stays roughly constant again for x above 0.6. The Young's modulus decreases with x in a nonlinear pattern.

The Poisson's ratio η of a materials represent an overall matric for the materials mechanical properties. The G/K ratio is inversely related to η. Their variation with x is plotted in **Fig. 5 (b)**. As can be expected, the variation with x is somewhat linear for $x < 0.5$ and $x > 0.75$. In between, where the subtle changes can occur as described above in the elastic coefficients and mechanical parameters, so are the Poisson's ratio and the G/K ratio. It has been generally accepted that for a pure and defect-free crystals, a material with low Poisson's ratio η (or high G/K ratio) tends to be more brittle and those with higher η will be less brittle. The calculated values for $Ti_2Al(C_xN_{1-x})$ solid solution follow this trend in transforming from a relatively ductile nitride phase in Ti_2AlN to a more brittle phase Ti_2AlC. **Fig. 5** also shows this trend in G/K as well with a transition crossover of the data at roughly x = 0.4 since G/K is inversely correlated with Poisson's ratio η, the more conventional parameter.

3.2 Electronic structure, and bonding and optical conductivity

We have also calculated the electronic structure and bonding in $Ti_2Al(C_xN_{1-x})$ solid solution for each x using the OLCAO method in the hope that they might shed some light on the subtle variations in their elastic and mechanical properties shown above. **Fig. 6** shows the calculated total density of states (DOS) for the 17 supercell models from x = 0 to x = 1. The zero of the energy in **Fig. 6** defines the Fermi energy which lies in the region of relatively low DOS, indicating to certain extent that these MAX phases should be stable from electronic structure perspective using free electron model[38]. It can also be seen that the peaks in the DOS shifts as x increases. For example, the lowest peak at - 15.0 eV is the N-2s peak for x = 0 (Ti_2AlN) and the lowest peak for x = 1 (Ti_2AlC) is at - 9.8 eV for the C-2s. In between, there are two such peaks which progressively evolve as x increases. In the upper valence band region (0 to -8 eV), the shifts of the peak structures are more complex, a reflection of the change in the bonding involving N-2p and C-2p orbitals. A noticeable observation is the relatively large low DOS region from -2.9 to -4.3 eV in Ti_2AlN. Below -2.9 eV, there are three noticeable peaks at -6.58, -4.96, and -4.52 eV respectively. Above these minimum, Ti_2AlN has a double peak at -1.87 and -1.36 eV. These structures progressively evolve as x increases. At Ti_2AlC, the DOS features in the range changed completely. Essentially, it has a sharp minimum of almost zero DOS at -2.13 eV with well-defined peak at –1.19 eV above and at -2.54 eV below the minimum. Such detailed evolution can only be revealed by detailed supercell calculations with large x values.

The atom resolved partial DOS (PDOS) for MAX phases is far more revealing on the electronic structure. However, presenting such results for all 17 supercell models is not practical. We selected four x values in the solid solution series for illustration. x = 0 and 1, the end members and x = 0.5 and 0.812, the intermediate x values where some interesting change in the mechanical properties occur as discussed above. They are plotted in **Fig. 7**. In **Table 3**, we also list the values of the DOS at the Fermi level, or $N(E_F)$ and the contributions from each type of atom. Note that these values corresponding to supercell so to convert the value to the unit cell, they need to be divided by 16. As is well known, most of the states at the E_F in MAX phases come from the d orbitals of transition metal M. This is certainly true for the $Ti_2Al(C_xN_{1-x})$ solid solution. The contribution from either N or C are almost negligible. From **Table 3,** it shows that the total DOS at Fermi level decreases as x increases. For x = 0 and x = 0.5, the $N(E_F)$ values are almost the same. The interesting point is that the contribution from Ti at x = 0.5 is actually larger than that of Ti_2AlN (x = 0).

We have also calculated the Mulliken effective charge Q* and the bond order (BO) according to the equations (1) and (2) in Section 2. The Q* values give us the charge transfer ΔQ* for each types of atoms. The variation of $\Delta Q^* = Q^o - Q^*$ where Q^o is the charge on the neutral atom is displayed in **Fig. 8 (a).** Both Ti and Al lose charge to N and C. It slightly increases in case of Ti but slightly deceases in Al with increasing x. The BO value between each pair of atoms is a quantitative measure of the relative strength of a bond. The total BO (TBO) of a crystal is the sum of all the bond order values in that crystal. When the TBO is divided by the volume of the crystal, we have the total bond order density (TBOD). The TBO can also be divided into different pairs: Ti-C, Ti-N, Ti-Ti and Al-Al. The directionality of these bonds could also affect the stability and variations mechanical parameters of the solid solutions. In **Fig. 8(b),** we plot the TBO in $Ti_2Al(C_xN_{1-x})$ solid solution as a function of x. It steadily increases as x increases reflecting the stronger T-C bonds compared to Ti-N bonds. We also note that the variations at small x (N-rich) and at large x (C-rich) are linear but with slightly different slopes. The two straight lines intercept at x = 0.5.

The calculated frequency-dependent real part of the optical conductivity $\sigma_1(\hbar\omega)$for the $Ti_2Al(C_xN_{1-x})$ solid solution is shown in **Fig. 9.** For the end members x = 0 and x = 1. The results are similar to those of ref. [39]. It can be seen that the main absorption peak in the conductivity at about 4.9 eV in Ti_2AlN (x = 0) start to shift to lower energy at x = 0.5 and a new broader peak structure began to develop at x > 0.75 at about 6 eV which becomes fully developed at Ti_2AlC (x = 1.0). All, these indicate the subtle changes in the electronic structure also affect the optical conductivity spectra as x changes.

3.3 Discussion

The above results firmly establish the trends in a continuous variation of solid solution composition x from Ti_2AlN to Ti_2AlC using rigorously *ab initio* calculations on stoichiometric supercell models. It is instrumental to compare these trends with what have been reported in the literature on the limited data on $Ti_2Al(C_xN_{1-x})$ solid solutions. Before we proceed, several facts must be emphasized. Firstly, there is no measured data for a continuous variation in x. Most of the available data we are aware of are on $Ti_2AlC_{0.5}N_{0.5}$, or x = 0.5[7-9]. Second, It is unrealistic to expect a close agreement between measured data and our simulation because the samples for

the MAX solid solutions are plagued with the problems of substoichiometry, presence of defects or vacancies at X or Al sites and porosity. Thirdly, the present supercell calculation, despite being the first for such realistic calculation, may still not be large enough to account for the subtleties related to the MAX solid solutions. Nevertheless, these data certainly provide the overall trend for the properties transition from a pure stoichiometric Ti_2AlN phases to another pure Ti_2AlC phase with sequential substation of N by C and vice versa.

It is interesting to point out that an early paper in 1996 by Piezka and Schuster[5] that preparation of continuous solid solution for $Ti_2Al(C_xN_{1-x})$ for x = 0.0 to 0.8 at 1490C appear to be difficult beyond x = 0.8. This may be correlated with the greater change in the lattice constant c and variations in the elastic and mechanical properties we simulated above this x values. For example, there is a crossover of the elastic coefficient C13 and C12 at x = 0.815 as pointed out in Section 3,1. The near linear relationship in variation of lattice constant *a* and *c* for x < 0.6 including the uptake of a for x > 0.6 shown in **Fig.3** appears to be in very good agreement with the data shown by Cobioch[9]**.** Reference **9** is the only work we can locate where in there are measurements at x = 0.0, 0.25, 0.5 0,75 and 1.0. Despite the fact that samples used in these measurements contain porosity or grossly nonstoichiometry for $Ti_2Al(C_x,N_{1-x})_y$ for $y \neq 1$. It is gratifying to see that the data for y =1, the trends for the change in *a* and *c* are consistent with our simulate data shown in **Fig. 3(a).**

The measurement for electronic structures in $Ti_2Al(C_xN_{1-x})$ solid solutions is even less than the lattice constant an mechanical properties. Scabarozi et al.[8] carried a specific heat measurement at constant volume for x = 0.5 sample and deduced through electron-phonon coupling constant that the $N(E_F)$ at x = 0.5 is significantly larger than x = 0 or 1. This seems to be not directly supported by the simulation data shown in **Table 3.** However, the calculated data did show that the Ti component of the DOS at Fermi level is the greatest at x = 0.5. It is more likely that the $N(E_F)$ used in the analysis should be more likely from the 3d electrons of the metal component, or Ti. Despite of some obvious disagreements, our calculations using a single method for continuous variation in x is quite illuminating in giving the overall trends.

4. Conclusions

We have carried out a detailed calculation on the $Ti_2Al(C_{1-x}N_x)$ solid solution using large supercells in order to answer some of the pressing questions. It is fairly clear that for this solid solution, the mechanical properties vary continuously with x between Ti_2AlN and Ti_2AlC with no evidence strengthening beyond the end members. They do have subtle variations for x > 0.5 which are supported by some existing experimental reports. This does not rule out the possibility of strengthening MAX phases in other solid solutions with substitutions in "M" or "A" elements. This is the first time that such large calculations using supercells for MAX solid solutions have been attempted. It is quite obvious that similar approach can be extended to other solid solutions and also used to study vacancies, porosities, formation of oxynitirdes in $Ti_2Al(C_xN_yO_z)$ etc. Such simulations will require even larger supercells but is clearly within our research if sufficient resources can be obtained.

There are ample evidences that many of the samples in the measurement for $Ti_2Al(C_{1-x}N_x)$ solid solution have sub-stoichiometry at the X and A sites. This implies that the calculations

performed on stoichiometric perfect sample can be used as a guideline in the limit of ideal situation. In this respect, repeated measurement on high quality and dense samples will be extremely valuable.

Finally, the fundamental question raised on the difference between MAX carbide and MAX nitrides cannot be explained in simple terms by detailed study for the $Ti_2Al(C_{1-x}N_x)$ solid solution alone because of the complex interplay of many contributing factors. It remains to be seem if statistical approach of data mining will be able to reach this goal. We still cannot resolve the general issue of why there are more MAX carbides than nitrides since the current study covers two existing end members in the series. We can only show the intrigue and subtle differences in their mechanical properties. A broad genomic approach use larger data base in seeking global correlation may help[2].

Acknowledgements

* This work was supported by National Energy Technology Laboratory (NETL) of the U.S. Department of Energy (DOE) under Grant No. DE-FE0005865. This research used the resources of the National Energy Research Scientific Computing Center (NERSC) supported by the Office of Basic Science of DOE under Contract No. DE-AC03-76SF00098.

Table 1. Total Energy dispersion with 10 models for each x. Energy is in eV and σ is standard deviation.

x	Smallest E	Mean	σ
0.062	-1029.2448	-1029.2296	0.0230
0.125	-1027.5354	-1027.4447	0.0595
0.188	-1025.7350	-1025.6525	0.0629
0.250	-1023.9482	-1023.8410	0.0792
0.312	-1022.0858	-1021.9424	0.1000
0.375	-1020.1519	-1020.0183	0.0995
0.438	-1018.2722	-1018.0161	0.1533
0.500	-1016.2020	-1016.0403	0.1014
0.562	-1014.1907	-1013.9866	0.1862
0.625	-1012.1220	-1011.9454	0.1429
0.688	-1010.1013	-1009.8058	0.1342
0.750	-1007.8392	-1007.6485	0.1067
0.812	-1005.5644	-1005.4777	0.0814
0.875	-1003.3251	-1003.2511	0.0711
0.938	-1000.9244	-1000.8834	0.0325

Table 2. Calculated elastic coefficients and mechanical parameters of $Ti_2Al(C_{1-x}N_x)$.

X	C_{11}	C_{33}	C_{44}	C_{66}	C_{12}	C_{13}	K	G	E	η	G/K
0.000	314.94	292.58	128.57	122.44	71.87	94.96	160.67	119.38	287.05	0.202	0.743
0.062	315.04	290.06	128.15	123.02	69.16	93.07	158.97	119.61	286.88	0.199	0.752
0.125	314.69	288.32	127.84	123.64	67.50	91.65	157.70	119.75	286.68	0.197	0.759
0.188	313.41	286.98	127.26	123.51	66.26	90.00	156.26	119.56	285.79	0.195	0.765
0.250	310.73	285.45	126.92	122.99	64.36	89.33	154.77	119.06	284.27	0.194	0.769
0.312	307.31	282.14	125.76	122.33	62.40	88.44	152.81	118.01	281.55	0.193	0.772
0.375	303.49	279.61	124.70	121.42	60.57	88.20	151.16	116.84	278.71	0.193	0.773
0.438	300.31	277.63	123.77	120.81	59.20	87.68	149.70	115.94	276.44	0.192	0.774
0.500	297.78	275.63	122.34	119.71	58.64	86.18	148.12	114.95	273.99	0.192	0.776
0.562	297.83	275.09	120.89	119.11	59.90	83.24	147.06	114.67	273.04	0.191	0.780
0.625	298.71	274.85	119.33	118.56	61.92	79.46	145.99	114.56	272.41	0.189	0.785
0.688	300.42	275.20	117.94	117.86	64.82	75.45	145.24	114.58	272.16	0.188	0.789
0.750	301.98	274.99	116.22	117.56	67.03	72.18	144.55	114.38	271.53	0.187	0.791
0.812	303.48	274.63	114.54	117.64	68.64	69.21	143.83	114.23	270.96	0.186	0.794
0.875	304.92	274.14	112.78	118.38	68.79	66.81	143.02	114.14	270.47	0.185	0.798
0.938	305.64	272.54	110.68	119.00	67.84	65.02	141.93	113.70	269.21	0.184	0.801
1.000	305.34	269.46	108.62	119.16	66.69	63.26	140.47	112.92	267.17	0.183	0.804

Table 3. Calculated DOS at Fermi level $N(E_F)$ (in unit of states/eV-supercell) and its atom resolved components for x = 0 (Ti_2AlN), x = 0.5 ($Ti_2AlC_{0.5}N_{0.5}$), x = 0.815 and x = 1 (Ti_2AlC).

x	Total	Ti	Al	N	C
0.000	**61.2812**	**47.7525**	**11.3000**	**2.2287**	**0.0000**
0.500	**60.5538**	**49.9930**	**9.2121**	**0.7471**	**0.6016**
0.812	**45.2068**	**35.5242**	**8.5617**	**0.2162**	**0.9047**
1.000	**43.0831**	**33.6386**	**8.2667**	**0.0000**	**1.1778**

Figure Captions:

Figure 1. Ball and stick illustration of the 4 x 4 x 1 supercell of $Ti_2AlC_xN_{1-x}$ solution. Left: x = 0 (Ti_2AlC); middle: x = 0.5 ($Ti_2AlC_{0.5}N_{0.5}$); right: x = 1 (Ti_2AlN). Grey, Ti atoms; Blue, C atoms; red, N atoms; pink, Al atoms.

Figure 2. Variation in standard deviation (σ) in eV with increased C concentration (x).

Figure 3. Top: variation of supercell lattice constants a and c in $Ti_2AlC_xN_{1-x}$ solid solution; bottom: change in cell volume as function of x.

Figure 4. Variation of the elastic constants of $Ti_2AlC_xN_{1-x}$ solid solution as a function of x.

Figure 5. Top: Variations of the mechanical bulk properties (K, G, and E) (Top); Poisson's ratio η and G/K (bottom) of $Ti_2AlC_xN_{1-x}$ solid solution as a function of x.

Figure 6. Calculated total density of states (TDOS) of $Ti_2AlC_xN_{1-x}$ solid solution.

Figure 7. Calculated partial density of states (PDOS) of $Ti_2AlC_xN_{1-x}$ solid solution for x = 0, 0.5, 0.815 and 1.

Figure 8. (a) Variation of calculated charge transfer for Ti, Al, N and C with x in $Ti_2AlC_xN_{1-x.}$ (b) Variation of total bond order in the supercell as a function x.

Figure 9. Calculated frequency-dependent optical conductivity in $Ti_2AlC_xN_{1-x}$ solid solution as a function of x.

References:

1. Barsoum MW. MAX Phases: Properties of Machinable Ternary Carbides and Nitrides: John Wiley & Sons; 2013.
2. Aryal S, Sakidja R, Barsoum MW, Ching WY. A genomic approach to the stability, elastic, and electronic properties of the MAX phases. physica status solidi (b). 2014;251(8):1480-97.
3. Service R. Computational science. Materials scientists look to a data-intensive future. Science (New York, NY). 2012;335(6075):1434.
4. Du Y, Sun Z, Hashimoto H, Barsoum M. Theoretical investigations on the elastic and thermodynamic properties of Ti< sub> 2</sub> AlC< sub> 0.5</sub> N< sub> 0.5</sub> solid solution. Physics Letters A. 2009;374(1):78-82.
5. Pietzka M A, Schuster JC. Phase Equilibria in the Quaternary System Ti-Al-C-N. Journal of the American Ceramic Society. 1996;79(9):2321-30.
6. Manoun B, Saxena S, Hug G, Ganguly A, Hoffman E, Barsoum M. Synthesis and compressibility of Ti3 (Al, Sn0. 2) C2 and Ti3Al (C0. 5, N0. 5) 2. Journal of applied physics. 2007;101(11):113523.
7. Radovic M, Ganguly A, Barsoum M. Elastic properties and phonon conductivities of Ti3Al (C0. 5, N0. 5) 2 and Ti2Al (C0. 5, N0. 5) solid solutions. Journal of Materials Research. 2008;23(06):1517-21.
8. Scabarozi T, Ganguly A, Hettinger J, et al. Electronic and thermal properties of Ti 3 Al (C 0.5, N 0.5) 2, Ti 2 Al (C 0.5, N 0.5) and Ti 2 AlN. Journal of Applied Physics. 2008;104(7):073713--6.
9. Cabioc'h T, Eklund P, Mauchamp V, Jaouen M. Structural investigation of substoichiometry and solid solution effects in Ti< sub> 2</sub> Al (C< sub> x</sub>, N< sub> 1− x</sub>)< sub> y</sub> compounds. Journal of the European Ceramic Society. 2012;32(8):1803-11.
10. Hu C, Zhang H, Li F, Huang Q, Bao Y. New phases' discovery in MAX family. International Journal of Refractory Metals and Hard Materials. 2013;36:300-12.

11. Yeh C L, and Chen JH. Combustion synthesis of (Ti1-xNbx)2AlC solid solutions from elemental and Nb2O5/Al4C3 containing powder compacts. Ceramic International 37 (2911) 3089-3094.
12. Yeh CL, and Wang WJ. Formation of MAX solid solutions $(Ti,V)_2AlC$ and $(Cr,V)_2AlC$ with Al_2O_3 addition by SHS involving aluminothermic reduction. Ceramic International 37 (2913) 7537-7544.
13. Kerdsongpana S, Buchholt K, Tengstrand O, Lu J, Jensen J J, Hultman L, and Eklund P. Phase stabilization and substrate effects on nucleation and growth of $(Ti,V)_{n+1}GeC_n$ thin film. J. Appl. Phys. 2011; 110:053516.
14. Naguib M, Bentzel C W, Shah J, et al., New solid solution MAX phases: $(Ti_{0.5},V_{0.5})_3AlC_2$, $(Nb_{0.5},V_{0.5})_2AlC$, $(Nb_{0.5},V_{0.5})_4AlC_3$, $(Nb_{0.8}, Zr_{0.2})_2AlC$. Mater. Res Lett., 2014; 2(4): 233-240.
15. Mockute A, Dallqvist M, Emmerlich J, Hutman L, Schneider JM, P.O.A, Persson and Rosen J. Synthesis and ab initio calculations of nanolaminated $(Cr,Mn)_2AlC$ compounds, Phys. Rev. B 2013; 87:094113.
16. Yu W, Shibo Li, Sloof WG. Microstructure and mechanic al properties of a Cr2Al(Si)C solid solution. Materials Science and Engineering A 2010; 527:5997-6001.
17. Bei G, Pedimonte BJ, Fey T, and Greil P. Oxidation behavior of MAX phases $Ti2Al_{(1-x)}Sn_xC$ solid solution. J. Am. Ceram. Soc., 2013; 96 (5) :1359-1362.
18. Yu w, Mauchamp V, Cabioc'h T, et al. Solid solution effect in the Ti2Al(CxNy) MAX phases, Synthesis, microstructure, electronic structure and transport properties. Acta Materialia 2014; 80:421-434.

19. Cabioc'h T, Eklund P, Mauchamp V and Jaouen M. Structural investigation of substiochiometry and solid solution effects in Ti2Al(C_x,N_{1-x})$_y$ compounds. J. Euro. Ceram. Sco., 2012;32:1803 -1833.
20. Vienna ab initio simulation package. Available Source: http://www. vasp. at. 2013.
21. Ching W. Theoretical studies of the electronic properties of ceramic materials. Journal of the American Ceramic Society. 1990;73(11):3135-60.
22. Ching W, Rulis P, Misra A. Ab initio elastic properties and tensile strength of crystalline hydroxyapatite. Acta Biomaterialia. 2009;5(8):3067-75.
23. Blöchl PE. Projector augmented-wave method. Physical Review B. 1994;50(24):17953.
24. Kresse G, Joubert D. From ultrasoft pseudopotentials to the projector augmented-wave method. Physical Review B. 1999;59(3):1758.
25. Perdew JP, Burke K, Ernzerhof M. Generalized Gradient Approximation Made Simple. Physical Review Letters. 1996;77(18):3865-8.
26. Perdew JP, Chevary JA, Vosko SH, et al. Erratum: Atoms, molecules, solids, and surfaces: Applications of the generalized gradient approximation for exchange and correlation. Physical Review B. 1993;48(7):4978.
27. Nielsen O, Martin RM. First-principles calculation of stress. Physical Review Letters. 1983;50(9):697.
28. Yao H, Ouyang L, Ching WY. Ab initio calculation of elastic constants of ceramic crystals. Journal of the American Ceramic Society. 2007;90(10):3194-204.
29. Voight W. Lehrbuch der Kristallphysik. Teubner, Leipzig. 1928;962.
30. Reus A. Berechnung der Fliessgrenze von Mischkristallen auf Grund der Plastizitätsbedingungen für Einkristall. Z. Angew. Math. Mech. 1929;9:49-58.
31. Hill R. The elastic behaviour of a crystalline aggregate. Proceedings of the Physical Society. Section A. 1952;65(5):349.
32. Mulliken RS. Electronic population analysis on LCAO–MO molecular wave functions. I. The Journal of Chemical Physics. 1955;23(10):1833-40.
33. Aryal S, Gao M, Ouyang L, Rulis P, Ching W. < i> Ab initio</i> studies of Mo-based alloys: Mechanical, elastic, and vibrational properties. Intermetallics. 2013;38:116-25.
34. Ching WY, Mo Y, Aryal S, Rulis P. Intrinsic Mechanical Properties of 20 MAX-Phase Compounds. Journal of the American Ceramic Society. 2013;96(7):2292-7.
35. Liang L, Rulis P, Ching W. Mechanical properties, electronic structure and bonding of α-and β-tricalcium phosphates with surface characterization. Acta biomaterialia. 2010;6(9):3763-71.
36. Aryal S, Rulis P, Ouyang L, Ching W. Structure and properties of the low-density phase ι-Al 2 O 3 from first principles. Physical Review B. 2011;84(17):174123.
37. Dharmawardhana C, Misra A, Aryal S, Rulis P, Ching W. Role of interatomic bonding in the mechanical anisotropy and interlayer cohesion of CSH crystals. Cement and Concrete Research. 2013;52:123-30.
38. Wang L, Mo Y, Rulis P, Ching W. Spectroscopic properties of crystalline elemental boron and the implications on B 11 C–CBC. RSC Advances. 2013;3(47):25374-87.
39. Adhikari P, Wen AM, French RH, et al. Electronic Structure, Dielectric Response, and Surface Charge Distribution of RGD (1FUV) Peptide. Scientific reports. 2014;4.
40. Poudel L, Rulis P, Liang L, Ching W. Electronic structure, stacking energy, partial charge, and hydrogen bonding in four periodic B-DNA models. Physical Review E. 2014;90(2):022705.
41. Liang L, Rulis P, Ouyang L, Ching W. Ab initio investigation of hydrogen bonding and network structure in a supercooled model of water. Physical Review B. 2011;83(2):024201.
42. Li N, Sakidja R, Aryal S, Ching W-Y. Densification of a continuous random network model of amorphous SiO 2 glass. Physical Chemistry Chemical Physics. 2014;16(4):1500-14.

43. Cover M, Warschkow O, Bilek M, McKenzie D. A comprehensive survey of M2AX phase elastic properties. Journal of Physics: Condensed Matter. 2009;21(30):305403.
44. Holm B, Ahuja R, Li S, Johansson B. Theory of the ternary layered system Ti–Al–N. Journal of applied physics. 2002;91(12):9874-7.
45. Sun Z, Li S, Ahuja R, Schneider JM. Calculated elastic properties of M< sub> 2</sub> AlC (M= Ti, V, Cr, Nb and Ta). Solid state communications. 2004;129(9):589-92.
46. Lofland S, Hettinger J, Harrell K, et al. Elastic and electronic properties of select M 2 AX phases. Applied physics letters. 2004;84(4):508-10.
47. Nagel S, Tauc J. Nearly-free-electron approach to the theory of metallic glass alloys. Physical Review Letters. 1975;35(6):380.
48. Mo Y, Rulis P, Ching W. Electronic structure and optical conductivities of 20 MAX-phase compounds. Physical Review B. 2012;86(16):165122.

Figures:

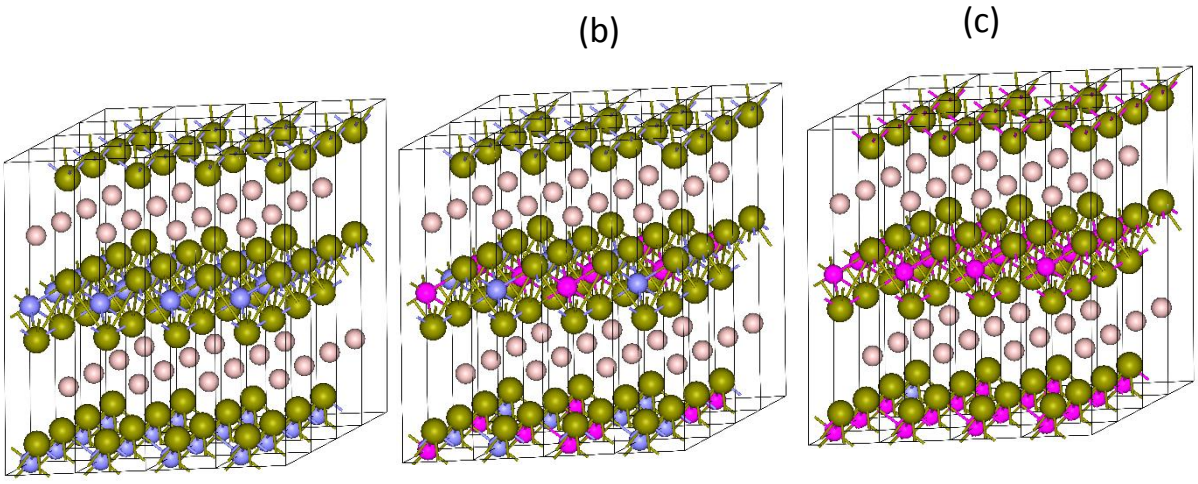

Figure 1. Representative ball and stick diagrams of 4 x 4 x 1 supercell of $Ti_2AlC_xN_{1-x}$ solution. Left only C, middle 50 % C and 50 % N and right only N.

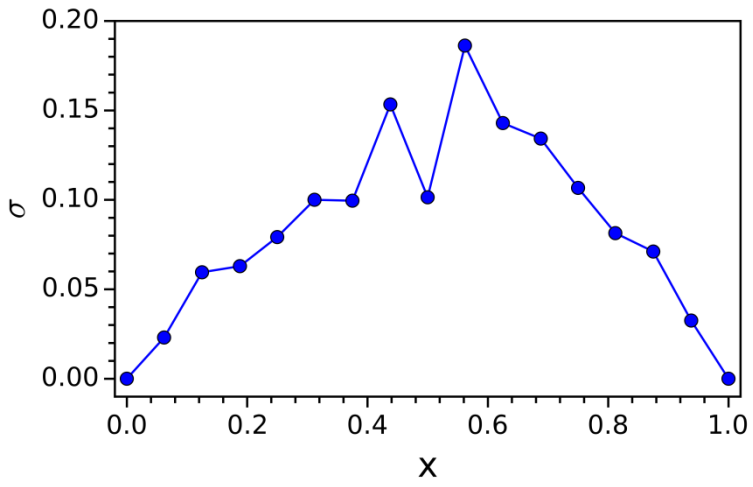

Figure 2. Variation in standard deviation (σ) in eV with increased C concentration (x).

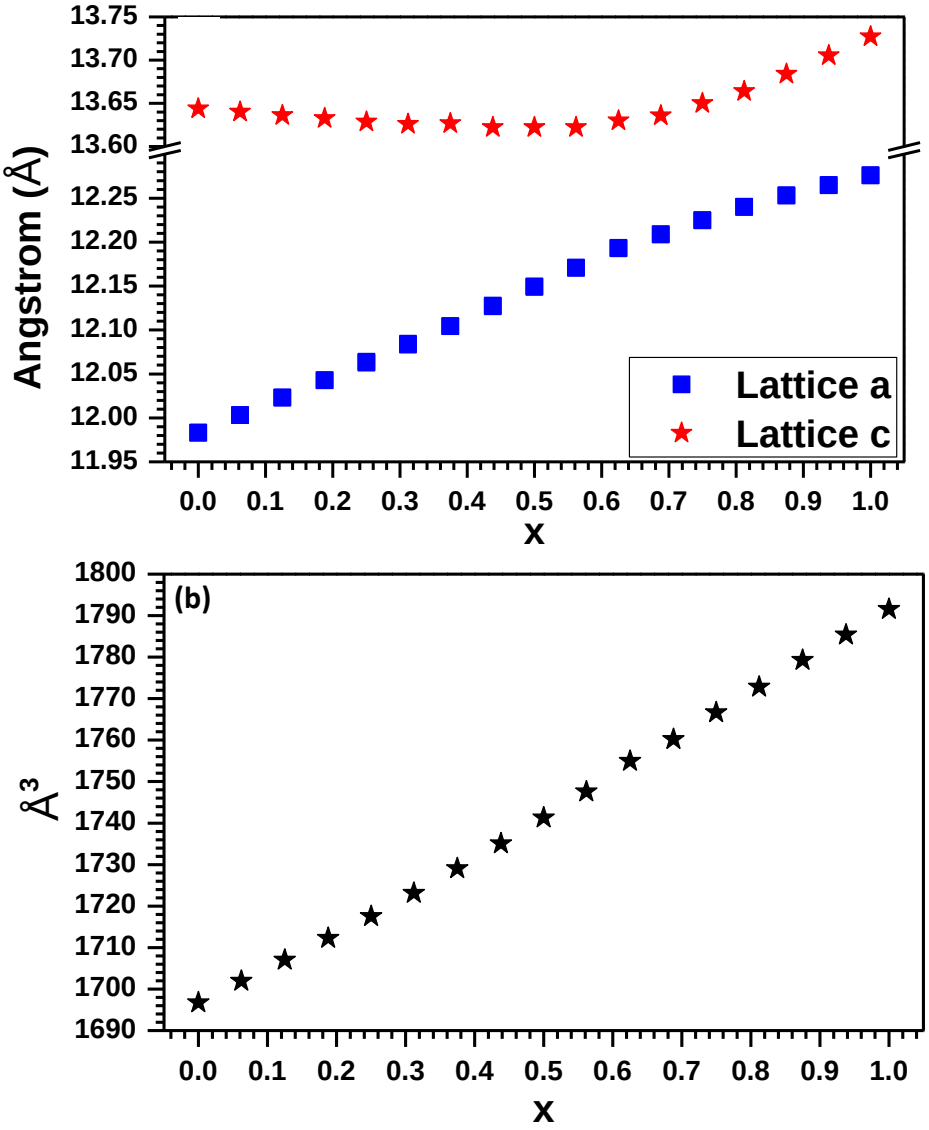

Figure 3. Change in lattice constants in $Ti_2AlC_xN_{1-x}$ solid solution (top) and volume (bottom).

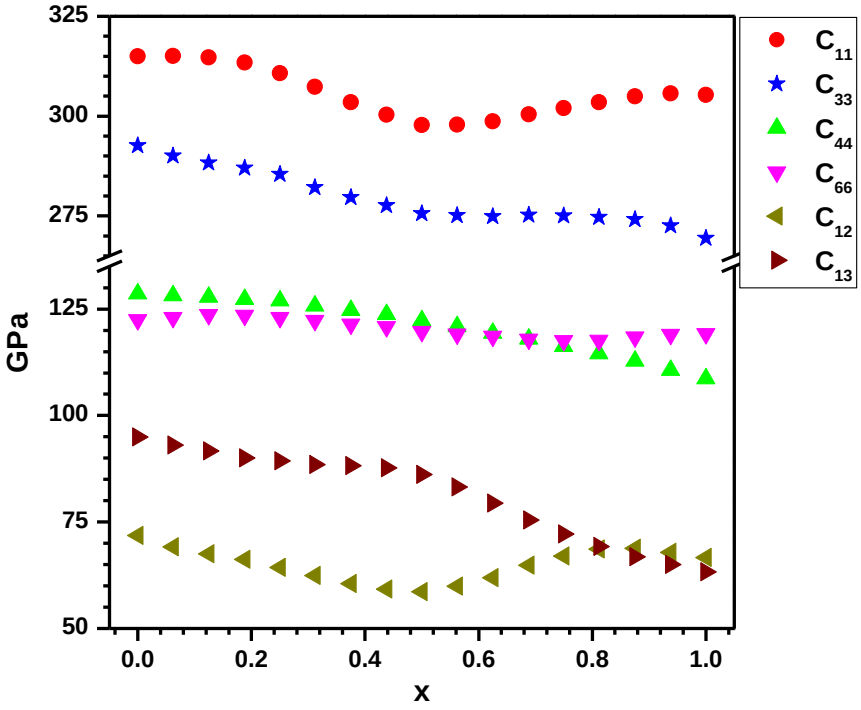

Figure 4. Elastic constants of $Ti_2AlC_xN_{1-x}$ solid solution plotted with x along the x-axis.

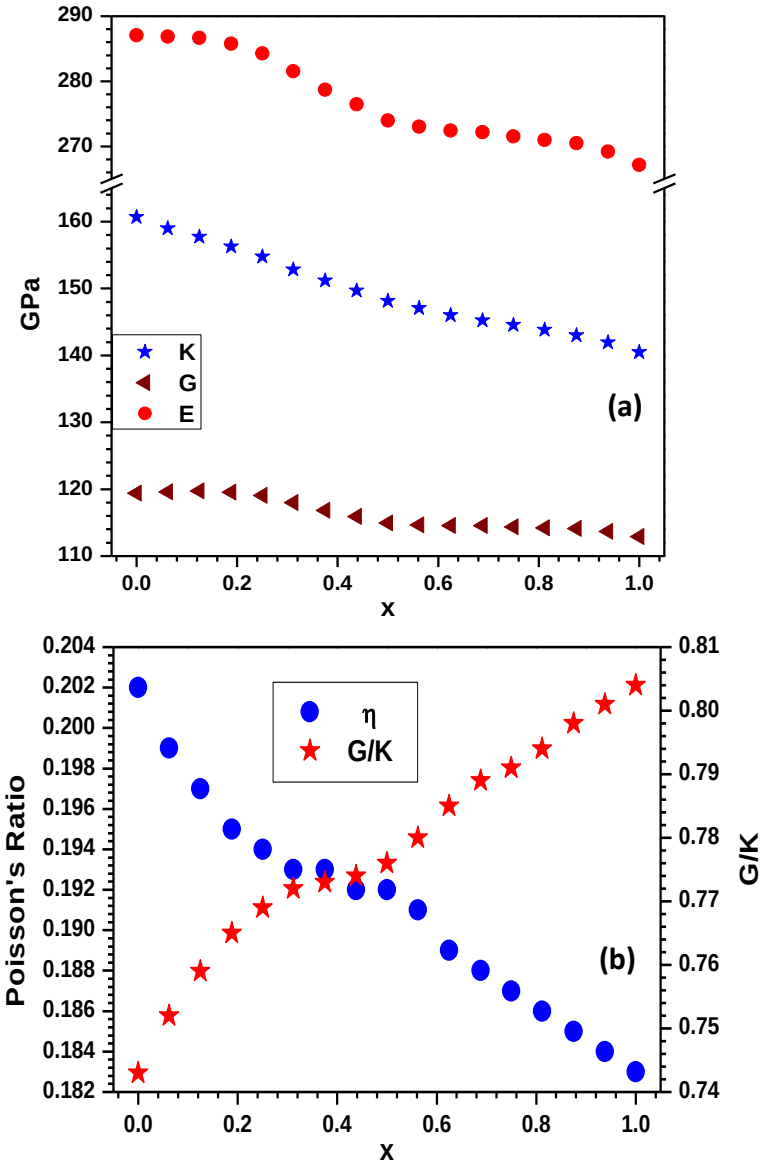

Figure 5. (Top) The mechanical bulk properties of $Ti_2AlC_xN_{1-x..}$ (Bottom) Poisson's ratio and G/K.

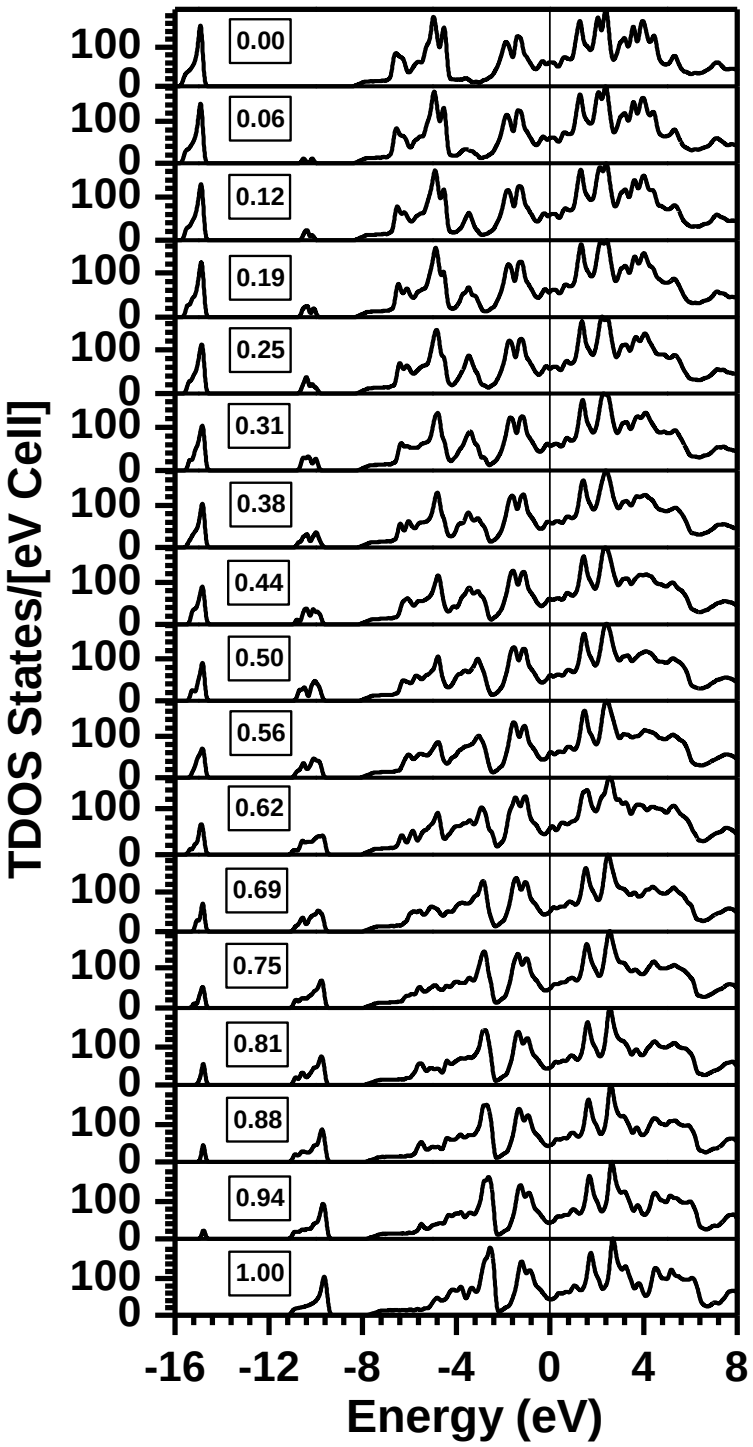

Figure 6. Total density of states (TDOS) of $Ti_2AlC_xN_{1-x}$ solid solution. The number in box represent x.

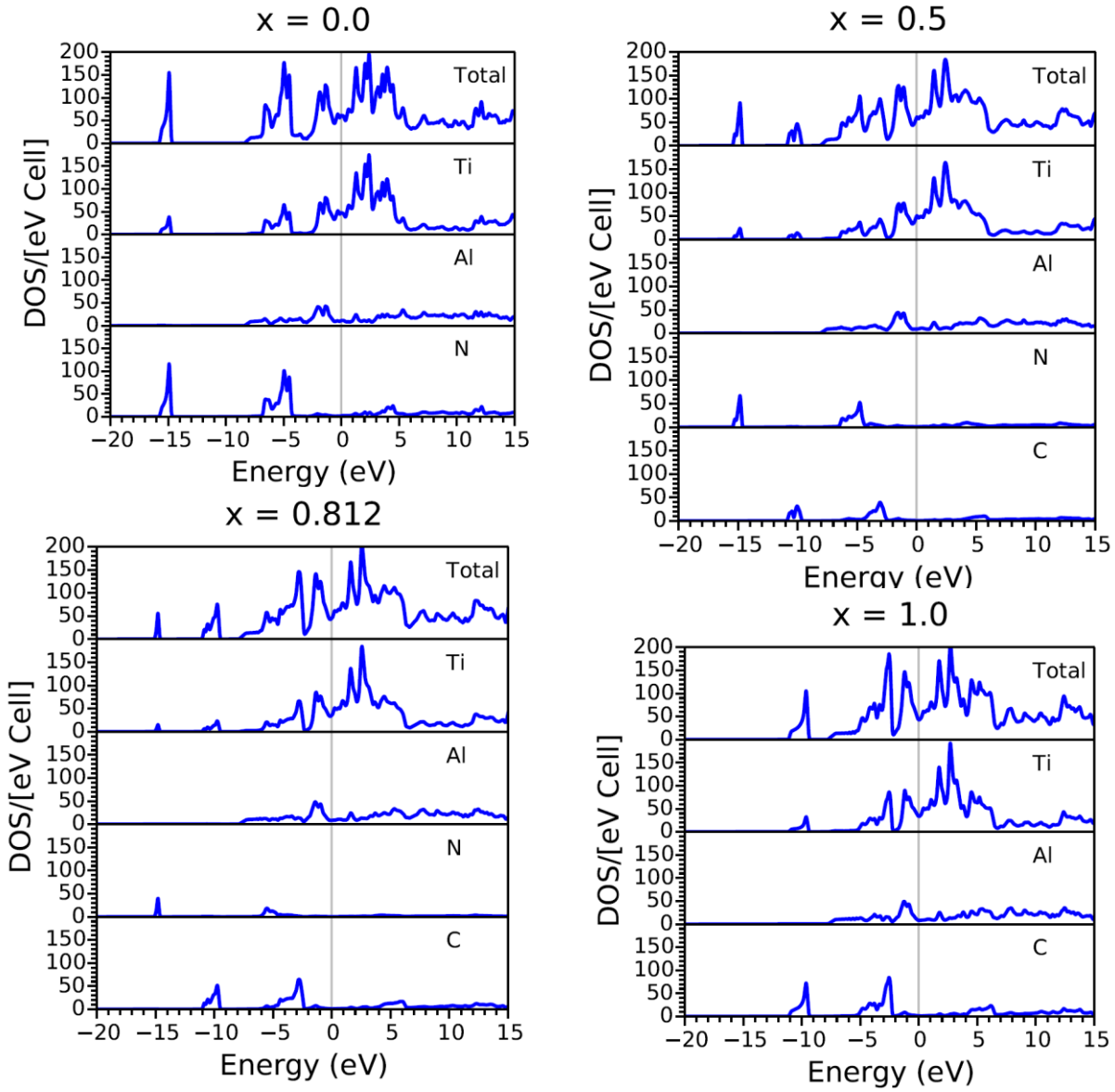

Figure 7. Total and partial density of states (DOS) in x=0.000, 0.500, 0.812, and 1.000. Top panel in each figure is total for that structure and bottom panels show atom resolved partial DOS.

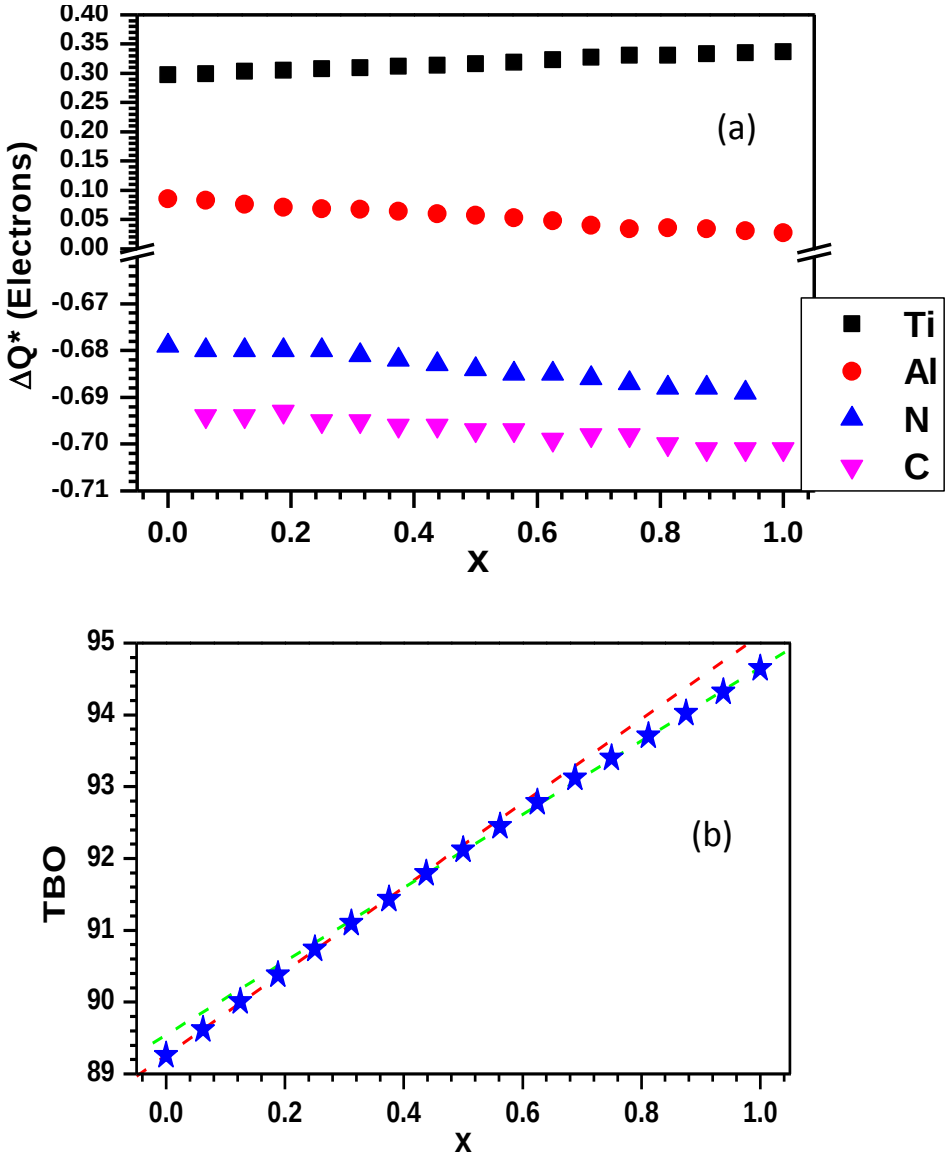

Figure 8. (a) Variation of calculated charge transfer for Ti, Al, N and C with x in $Ti_2AlC_xN_{1-x}$. (b) Variation of total bond order in the supercell as a function x.

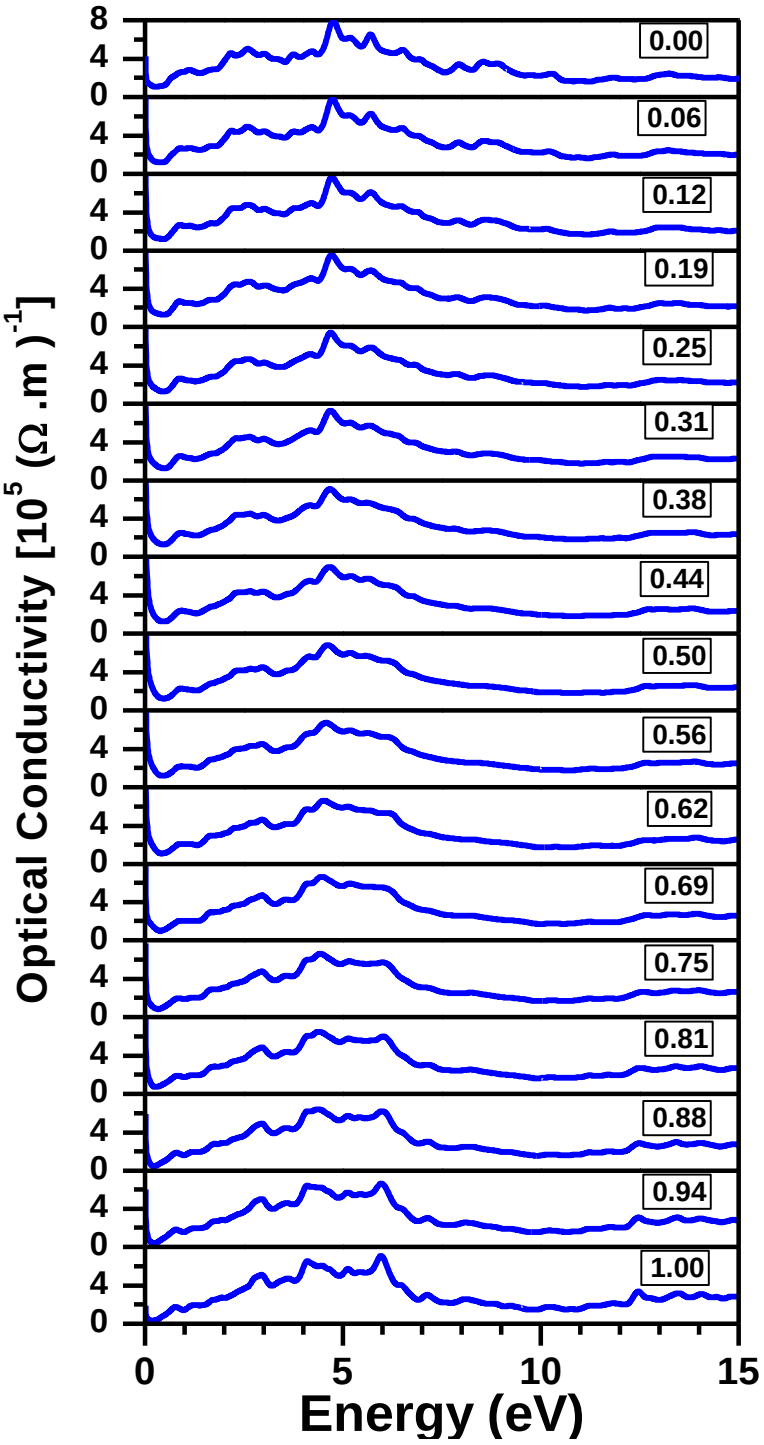

Figure 9. Frequency dependent averaged optical conductivity of $Ti_2AlC_xN_{1-x}$ solid solution.